Journal of Hydrology: Regional Studies 49 (2023) 101516

Contents lists available at ScienceDirect

Journal of Hydrology: Regional Studies

journal homepage: www.elsevier.com/locate/ejrh

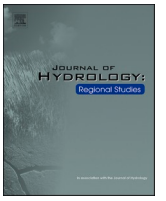

Investigating the warming effect of urban expansion on lake surface water temperature in the Dianchi lake watershed

Yi Luo [a,b], Linfeng Tang [a,b,*], Kun Yang [a,b,*], Xiaolu Zhou [c], Jing Liu [a,b], Yang Zhang [a,b], Zongqi Peng [a,b]

[a] Faculty of Geography, Yunnan Normal University, Yunnan 650500, China
[b] GIS Technology Research Center of Resource and Environment in Western China, Ministry of Education, Yunnan Normal University, Yunnan 650500, China
[c] Department of Geography, Texas Christian University, 2850 University Drive, Fort Worth TX76129, USA

ARTICLE INFO

Keywords:
Lake surface water temperature
Urban expansion
Impact mechanism
Warming effect

ABSTRACT

Study region: Dianchi lake (DCL) watershed, located in southwestern China, has undergone significant urbanization.
Study focus: Due to the accelerating urbanization in the watershed, the influence of urban expansion on lake surface water temperature (LSWT) has become increasingly significant. However, there is currently no quantitative study on the specific warming value of LSWT caused by urban expansion. This study primarily quantifies the increase in LSWT caused by urban expansion from two perspectives: the rise in near-surface air temperature (NSAT) resulting from urban expansion and the thermal runoff generated by urban expansion.
New hydrological insights for the region: We found that the DCL watershed experienced significant urban expansion between 2001 and 2018. In this context, the cumulative increase in LSWT caused by the newly added impervious surface (IS) through NSAT is about 0.25 °C. The cumulative warming of the newly added IS on the LSWT through thermal runoff is about 0.05–0.06 °C. Urban expansion mainly affects the LSWT by increasing the NSAT.

1. Introduction

Lakes play a vital role in regulating the regional climate, providing water resources for human production and life, and facilitating convenient transportation (Huziy and Sushama, 2017), forming an indispensable component of sustainable urban development (Yang et al., 2019). By 2030, China's economy is projected to experience rapid growth, leading to a population size of approximately 1.445 billion and an urbanization rate of around 70.12% (Sun et al., 2017). Urban expansion is one of the influencing factors of lake surface water temperature (LSWT), which, in turn, serves as a crucial physical parameter affecting lake water quality. The rapid expansion of urban areas within the watershed will have a considerable effect on the lake's ecology, including its biogeochemical processes and biological community(Chen et al., 2015; Hampton et al., 2008; O'Reilly et al., 2003; Peng et al., 2022; Sharma et al., 2007; Yang et al., 2020a).

LSWT is sensitive to climate change and human activities (Houser, 2006; Ptak et al., 2018; Woolway et al., 2020; Yang et al., 2020b). Shallow lakes, in particular, show a rapid response of LSWT to solar and atmospheric forcing (Du et al., 2020a). Existing

* Corresponding authors at: Faculty of Geography, Yunnan Normal University, Yunnan 650500, China.
E-mail addresses: tanglinfeng0940@163.com (L. Tang), yangkun@ynnu.edu.cn (K. Yang).

https://doi.org/10.1016/j.ejrh.2023.101516
Received 13 June 2023; Received in revised form 14 August 2023; Accepted 22 August 2023
Available online 27 August 2023

research results on many lakes show that air temperature is the most important factor affecting the LSWT(Schmid et al., 2014; Schmid and Koster, 2016; Yang et al., 2020b). However, research findings about LSWT in certain regions indicate that the rate of LSWT increase surpasses that of air temperature rise (Austin and Colman, 2007; Schmid and Koster, 2016; Woolway et al., 2019), and show that there are other important factors that contribute to the LSWT increase, such as urban expansion (Jia et al., 2022; Yang et al., 2020b). Although climate remains the primary influencing factor for lake surface water temperature (LSWT) in most lakes, the accelerating urbanization within the watershed has made the impact of urban expansion on LSWT increasingly significant and cannot be ignored.

The urban heat island effect, as many other urbanization impacts, have always been the focus of many research (Chen et al., 2022; Gu, 2019; Martinez-Zarzoso and Maruotti, 2011; Yao et al., 2021). According to prior studies, the maximum urban heat island intensity of major cities in the world is between 7 and 12 °C (Xu et al., 2021). Other scholars' research findings on 32 major cities in China demonstrate that the average annual heat island intensity in these cities ranges from 0.01 to 1.87 °C during the day and from 0.35 to 1.95 °C at night(Zhou et al., 2014). Based on quantitative research examining the relationship between urban expansion area and the specific temperature increase of near surface air temperature (NSAT), it has been observed that every 10% increase in urban spatial continuity contributes to a minimum temperature rise of the annual average Urban Heat Island effect by 0.3–0.4 °C (Debbage and Shepherd, 2015). Every 10% increase in urban expansion within 1 km around the meteorological station may result in a 0.13 °C increase in temperature recorded at the station (He et al., 2013). This indicates that a high percentage of IS is usually related to an elevated land surface temperature (Du et al., 2020b). At the same time, the heat exchange between air-water interfaces is one of the important ways to govern the temperature of the water surface(Zhao et al., 2020a). Consequently, as the air temperature in the watershed rises, heat exchange with the LSWT results in a continuous warming of the LSWT. In addition, cities generate more thermal runoff during their expansion process, which will have an impact on the LSWT. As urban expansion occurs, there is a significant increase in the area covered by artificial materials such as asphalt and concrete within the city. These materials have poor thermal performance and high absorption performance (Xu et al., 2021), facilitating thermal radiation and releasing higher heat. When

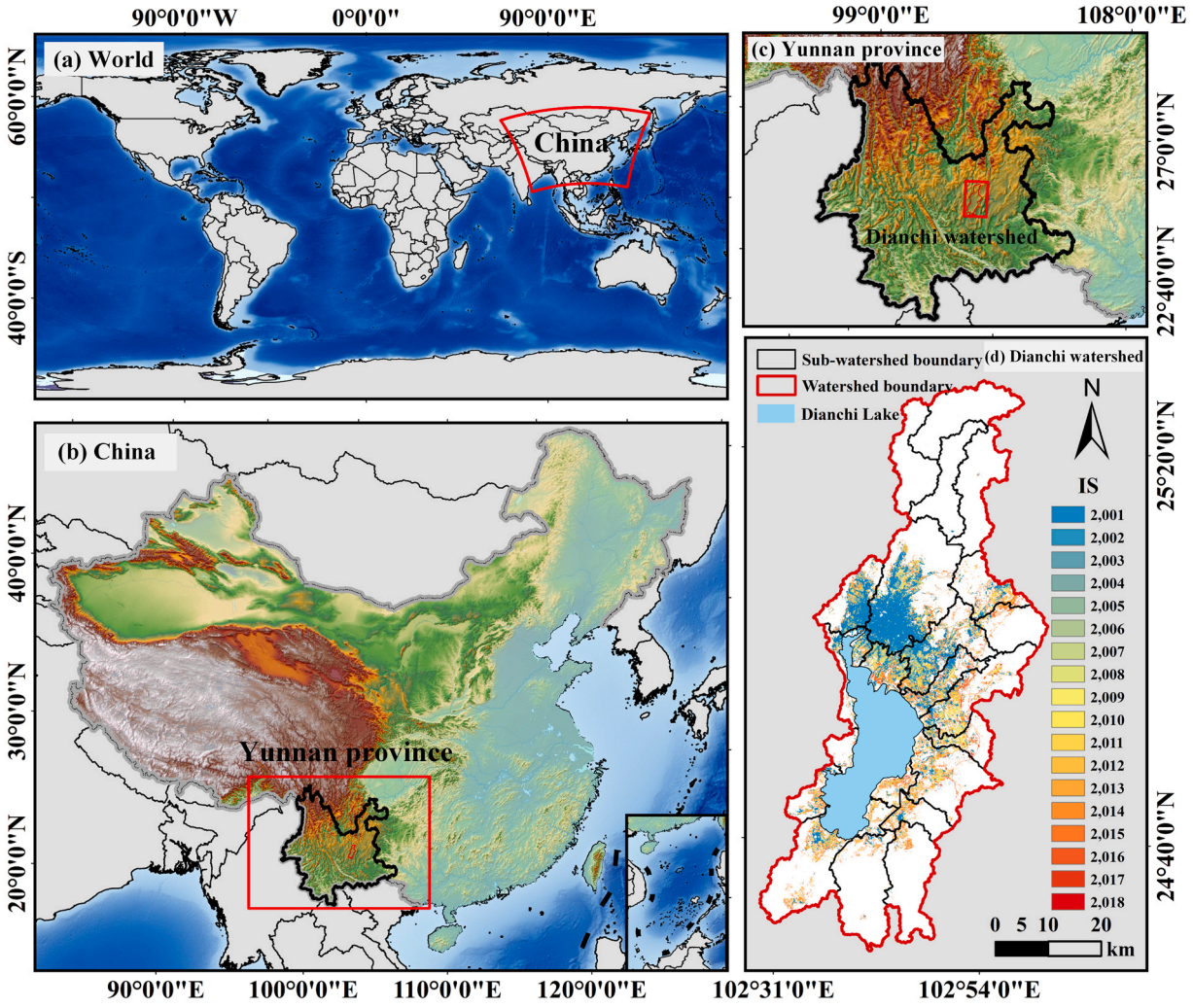

Fig. 1. Overview of the study area.

summer rainfall events occur, these stored heat will be transferred to the runoff, resulting in thermal runoff pollution(Buren et al., 2000; Herb et al., 2008; Kim and Sansalone, 2008; Ramier et al., 2011). As the main manifestation of urbanization, the alteration of impervious surface (IS) coverage is commonly utilized as a crucial measure to evaluate the extent of urban expansion(Luo et al., 2018). Therefore, studies have shown that when the coverage of IS in a watershed increases from 20% to 50%, it will lead to an increase in runoff temperature of 3 °C (Sabouri et al., 2013). For every 1% increase in the proportion of IS in the watershed, the temperature of urban runoff will increase by 0.09 °C(Galli, 1990; Janke et al., 2009; Sabouri et al., 2013). This thermal runoff will converge into the lake, leading to an increase in the LSWT.

Although there have been some studies on the impact of urban expansion on the LSWT, these studies only demonstrate that urban expansion affects the LSWT. The research methods used are often simple, such as correlation and regression analysis(Yang et al., 2020b; Yang et al., 2021). There is no quantitative study on the specific warming values of LSWT caused by urban expansion. Therefore, the research objective of this article is to elucidate the mechanisms by which urban expansion affects the LSWT, based on the integration of relevant fields and our team's research findings. On this basis, a research method will be designed to effectively quantify the actual temperature increase of LSWT caused by urban expansion. Previous studies have proved that the intensity of urban heat island in summer is higher than in winter (Zhou et al., 2014), and the land surface temperature in summer is also higher than that in other seasons. In addition, the rainfall in the study area is concentrated in summer, which will generate more thermal runoff. Summer is also the season with the greatest impact of IS on the LSWT. Therefore, summer is selected as the best time to explore the warming effect of IS expansion on LSWT.

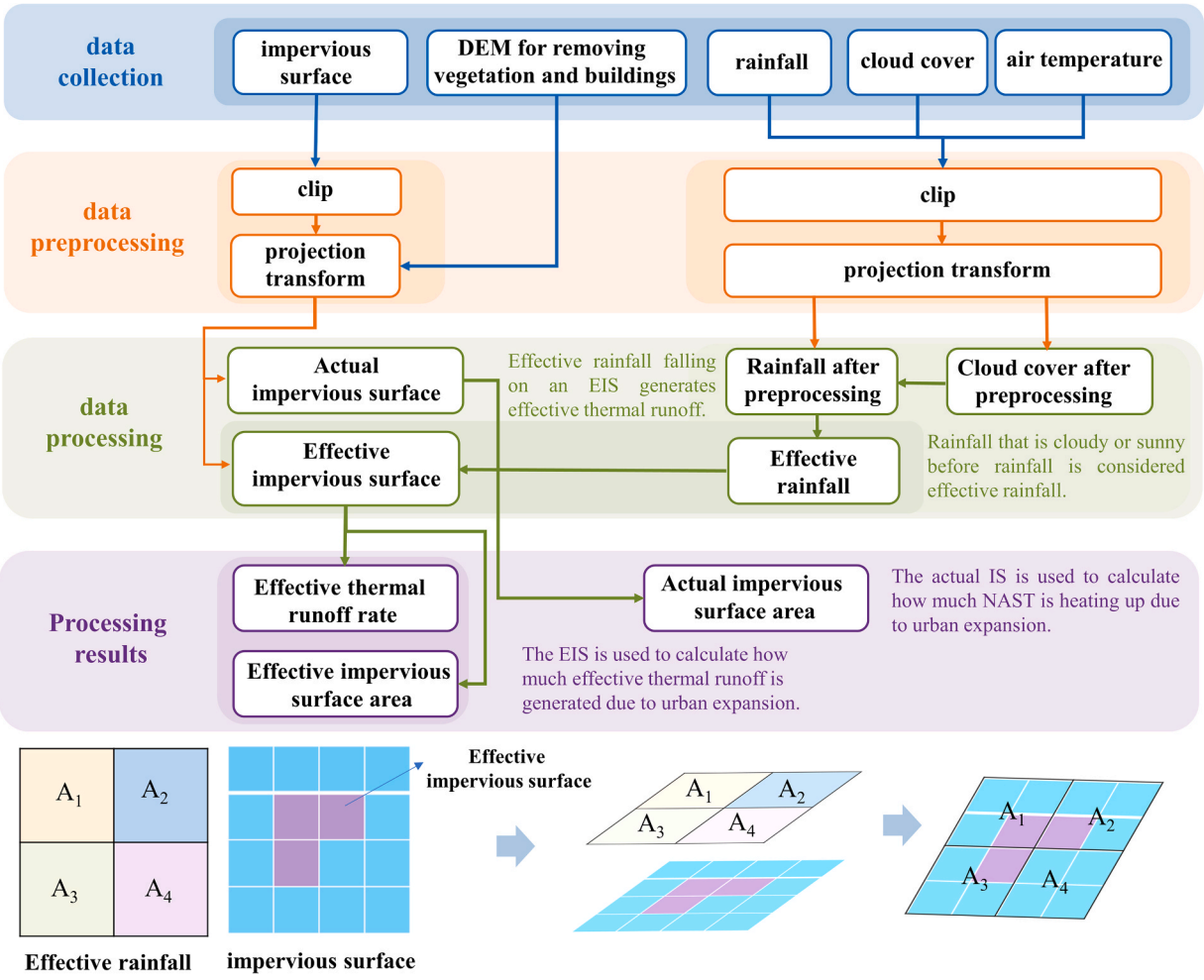

Fig. 2. Data processing flowchart.

2. Materials and methods

2.1. Study area

Located in southwest China, Dianchi Lake (DCL) is the largest freshwater lake in Yunnan Province and the sixth largest freshwater lake in China. The specific location is shown in Fig. 1. DCL has an average width of 7.2 km, an area of 297.90 km^2, an average depth of 1.93 m and a capacity of 11.69 $\times$ 10^8 m^3(Yang et al., 2020b). The climate in the DCL watershed belongs to a subtropical plateau monsoon climate, with dry and cool conditions in the winter half year and humid and warm conditions in the summer half year. The region receives most of its rainfall between May and October, with an average annual rainfall of 1000 ml and an average temperature of 14.8 °C. Due to economic development, cities within the DCL watershed have undergone substantial expansion. The impervious surface area (ISA) of the watershed in 2018 is 2.16 times bigger than that of 2001, and the growth rate of the IS is 237.29 km^2 /decade (Tang et al., 2022). Moreover, the IS in the watershed is gradually expanding along the DCL coast, which will have an important impact on the lake ecology in the DCL watershed (Luo et al., 2017).

2.2. Data source and processing

2.2.1. Data source

The data used in this paper mainly include IS, rainfall, cloud cover, NSAT, and DEM data with vegetation and urban buildings removed. The IS data we use is the IS dataset built by the Gong Peng team at Tsinghua University, with a spatial resolution of 30 m and an average accuracy rate of over 90% (Gong et al., 2020). This data can be downloaded from (http://data.ess.tsinghua.edu.cn/). Rainfall, cloud cover and NSAT data are ERA5 reanalysis hourly data of each single day from 1959 to present day. Many studies have proved that ERA5 reanalysis data is one of the best in process analysis products(Hersbach et al., 2020; Jiao et al., 2021; Tarek et al., 2020). These three data are downloaded from (https: //cds. climate. copernicus. eu /cdapp #! /dataset /reanalysis-era5-single-levels? Tab=form), where the rainfall data uses convective rainfall rate, which is the rainfall rate (rainfall intensity) at a specified time on the earth's surface. It is generated by the convection scheme in the ECMWF integrated forecasting system (IFS), with a spatial resolution of 0.25°. This data represents the rate of rainfall uniformly distributed on the pixel, and its unit is mm/s. The cloud cover data used in this paper is the total cloud cover, which represents the proportion of cloud cover in the pixel. It is calculated from the clouds at different model levels through the atmosphere. The data has a spatial resolution of 0.25° and includes cloud cover fractions ranging from 0 to 1. The NSAT data utilizes temperature readings taken at a height of two meters, measured in Kelvin. This data will be utilized in the calculation of thermal runoff temperature and LSWT. To determine the IS that can produce effective runoff, the DEM data excluding vegetation and building height will be employed. The resolution of this dataset is 30 m, and compared to other data, the average absolute vertical error of urban built-up areas in this dataset has decreased from 1.61 m to 1.12 m(Hawker et al., 2022). This data can be downloaded from (https://data.bris.ac.uk/data/dataset/25wfy0f9ukoge2gs7a5mqpq2j7).

2.2.2. Data processing

Fig. 2 shows the entire process of data processing in this study. First, the data used in this study was collected and preprocessed. Second, in the data processing and result processing stage, the main tasks are as follows: 1. Extract the actual ISA from the preprocessed IS data. 2. Extract effective impervious surfaces (EIS) by combining DEM data that remove vegetation and buildings and IS data. 3. Use the pre-processed cloud cover and rainfall data to extract effective rainfall. 4. Calculate the effective thermal runoff rate by combining effective rainfall and the EIS. The above processing principles are shown in Section 2.3.3.2.

It is important to highlight that EIS and effective rainfall have different resolutions. To address this, we utilize the boundary of effective rainfall (Low resolution data with a data resolution of 0.25°) to clip the EIS (High resolution data with a data resolution of 30 m), and the effective rainfall on all EIS within the same boundary will be calculated as the same. In other words, each low resolution grid covers multiple grids of high-resolution data, and when combining two data, the values of multiple high-resolution data within the same low resolution grid coverage range are considered the same. For example, in the lower half of Fig. 2, the effective rainfall on all EIS within the A1 range will be counted as the same.

2.3. Research methods

According to the existing research methods, it is not possible to directly calculate the exact increase in LSWT caused by urban expansion. However, both domestic and foreign studies, as well as our team's research results, indicate that urban expansion primarily affects LSWT through two ways: increasing NSAT and generating heat runoff. Therefore, we can first calculate how much the urban expansion leads to an increase in NSAT, as well as the amount of heat runoff generated during the urban expansion process. Then, we can calculate the extent to which the increased NSAT and heat runoff contribute to the warming of LSWT. In this way, we can indirectly calculate the increase in LSWT caused by urban expansion.

2.3.1. Pretreatment of impervious surface

Based on the IS data, we extracted the IS data of DCL watershed from 2001 to 2018 to study the increase of LSWT attributed to urban expansion from 2001 to 2018(When calculating the effect of NSAT on LSWT, the percentage change of IS in the watershed is considered. By comparing the IS in 2000, the percentage change of urban expansion in 2001 can be obtained). At the same time, considering that the IS data is the annual scale data, in order to ensure the data integrity, we used the meteorological conditions in the

following summer to calculate the increase of the LSWT caused by urban expansion.

2.3.2. Calculation of the increase of LSWT caused by near-surface air temperature

The following formula is used to calculate the portion of the impact on raising LSWT by urban expansion through increasing NSAT. The formula utilized is based on the findings of two distinct studies. The first, conducted by He et al. (2013), explored the influence of urban expansion on NSAT. The second study, conducted by Schmid et al. (2014), examined the energy conversion process between NSAT and LSWT. This formula is divided into two parts. The first part is used to calculate the temperature rise of the NSAT attributed to urban expansion in the watershed, and the second part is the energy conversion between the NSAT and the LSWT. By calculating the NSAT rise caused by urban expansion in the watershed, the effect of urban expansion on the LSWT can be further calculated.

$$T_{\mathrm{l}} = \frac{\sum_{i=1}^{\mathrm{n}} T_1 + T_2 + \cdots\cdots T_n}{n} \times P_t \tag{1}$$

$T_{1,\ 2.\ n}$ respectively represent the increase of NSAT caused by the expansion of IS in the 1st and 2nd. n sub-watersheds. For the calculation of the temperature increase of the NSAT caused by the expansion of the IS in the sub-watershed, He et al. (2013) found that every 10% increase in urban expansion within 1 km around the weather station will cause the temperature to rise by 0.13 °C. P_t represents the energy conversion between NSAT and LSWT. Research shows that the value of LSWT increase corresponds to 75–90% of the value of NSAT increase (Schmid et al., 2014; Schmid and Koster, 2016). According to the research results of Schmid et al. (2014) and the corresponding geographical location of DCL watershed in the research results of this scholar, P_t is determined as 80%.

2.3.3. Calculation of LSWT increase caused by thermal runoff

2.3.3.1. Thermal runoff warming formula. The warming formula of the thermal runoff to the LSWT can be used to calculate the part of the increase of the LSWT caused by urban expansion through thermal runoff. By calculating the amount of thermal runoff, the thermal runoff temperature and the lake temperature, the warming of the LSWT by the thermal runoff can be calculated by using the liquid mixing formula between different temperatures when the lake capacity is known.

$$T_r = \frac{C_{Thermalrunoff} \times T_{Thermalrunoff} + C_{lake} \times T_{lake}}{C_{Thermalrunoff} + C_{lake}} - T_{\mathrm{lake}} \tag{2}$$

$$C_{thermalrunoff} = C_{totalrainfall} - C_{effectiverainfall} - C_{infiltration} - C_{otherlosses} \tag{3}$$

T_r represents the warming of the thermal runoff to the LSWT. In the above formula, $C_{Thermal\ runoff}$ represents the amount of effective thermal runoff, $T_{Thermal\ runoff}$ represents the thermal runoff temperature, C_{lake} represents the lake capacity, and T_{lake} represents the lake water temperature. In the previous study, we established a fitting equation based on the water temperature and temperature of the nine plateau lakes in Yunnan Province, so the water temperature data in this paper is directly calculated based on the fitting equation(Yu, 2022). See 2.3.3.1–2.3.3.4 for the determination process of $C_{Thermal\ runoff}$. $C_{total\ rainfall}$ represents the total rainfall, $C_{effective\ rainfall}$ represents the rainfall that meets the conditions for generating thermal runoff, $C_{infiltration}$ represents the rainfall that flows into the permeable surface after falling to the IS, and $C_{other\ losses}$ represents the rainfall that is lost by other means.

2.3.3.2. Calculation of impervious surface capable of producing effective runoff. In this paper, Effective thermal runoff refers to the rainfall that lands on the IS and is not lost due to processes such as evaporation or infiltration. Instead, it ultimately accumulates and flows into the lake. In other words, effective thermal runoff equals to the rainfall minus runoff loss. Runoff loss is defined as the part of

Fig. 3. Determination principle of impervious surface capable of generating effective runoff.

rainfall that did not produce runoff and calculated as rainfall minus runoff (Ramier et al., 2011). The process of runoff loss includes evaporation, infiltration and temporary water storage on the surface (Ramier et al., 2011). In this paper, runoff loss includes not only evaporation, infiltration, and temporary water storage on the surface but also includes rainfall that does not meet the conditions for thermal runoff.

Since the spatial relationship between the IS and the permeable surface in the urban area will affect the generation of effective runoff, the land surface may not generate effective runoff after rainfall in the urban area. In this study, the identification of IS which is capable of generating effective runoff is based on the spatial relationship between permeable surfaces, IS, and their respective elevations. The specific principle is shown in Fig. 3. It can be seen from Fig. 3 that the relationship between the IS and the permeable surface can be divided into four categories. The first is that when the central pixel is the IS and the surrounding eight pixels are all permeable surfaces, no matter which direction the runoff flows to, it will eventually flow through the permeable surface and infiltrate, and the IS will thus be deleted. In the second case, when the central pixel is an IS, if any of the eight surrounding pixels has a permeable surface and the elevation is lower than the middle pixel, the central pixel will be deleted, otherwise the middle pixel will be retained. The third case is that when the central pixel is a permeable surface and the eight surrounding pixels have an IS, if the elevation of the IS is higher than the elevation of the middle pixel, the IS pixel will be deleted, otherwise, it will be retained. The fourth case is that when the middle pixel and the surrounding pixel are both IS, all IS pixels will be retained.

2.3.3.3. Determination of rainfall that can produce effective runoff. Apart from the loss of runoff through infiltration of permeable surfaces, the formation of thermal runoff also requires more stringent conditions. The occurrence of thermal runoff relies on specific weather conditions, e.g., sunny, or cloudy conditions in which the IS absorbs sufficient heat before rainfall. To identify rainfall events that result in effective runoff, cloud data is combined with rainfall event data for screening purposes. According to Liu et al. (2022), the division theory of sunny, cloudy and overcast days, when the amount of clouds in the sky is 0–30%, it is classified as sunny, 30–70% is classified as cloudy, and more than 70% is classified as overcast. We associated the rainfall data with the weather condition one hour before the rainfall, removed the rainfall data that was overcast one hour before the rainfall, and retained the rainfall data that was sunny or cloudy one hour before the rainfall. Retention of this part of rainfall data is considered to be rainfall that can generate thermal runoff.

2.3.3.4. Other losses. Apart from the rainfall infiltrating the permeable surface, the rainfall that falls on the IS also experiences losses due to evaporation, a small amount of infiltration and temporary surface water storage. To assess the proportion of this loss, Ramier et al. (2011) studied surface evaporation, small infiltration and surface temporary water storage on two streets. After measuring the rainfall and runoff flow in these areas, their findings revealed that this component of runoff loss accounted for 30–40% of the total rainfall.

2.3.3.5. Determination of thermal runoff temperature. The research area of this paper is the DCL watershed, which is part of Kunming,

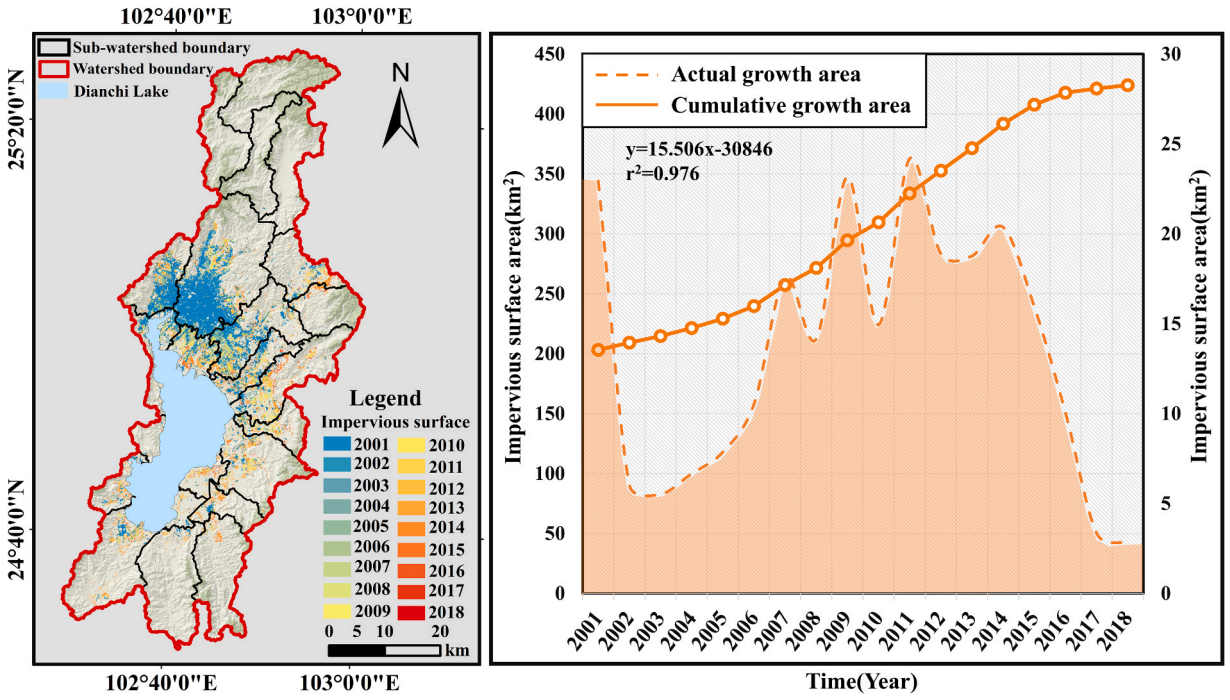

Fig. 4. Temporal and spatial changes of effective impervious surface.

the capital of Yunnan Province. Most of the buildings in Kunming are concrete structures, while asphalt and other ISs only account for a small part of the total IS. Therefore, we approximate the IS of the entire DCL watershed as concrete surfaces in order to calculate the increase in LSWT caused by urban expansion. Through the micro-scale study conducted by our team in the DCL watershed, we have determined the thermal runoff temperature that can be generated by the IS of concrete (Luo et al., 2019; Luo et al., 2023). Luo et al. (2023) conducted a micro-scale study in the DCL watershed in summer. The results indicated that the thermal runoff temperature stabilized after a rise of 1.62 °C compared to the initial rainfall temperature. Therefore, in this paper, we set the thermal runoff temperature as 1.62 °C higher than the initial rainfall temperature.

3. Results

3.1. Temporal and spatial variation of impervious surface capable of generating effective runoff

We define the IS that can produce effective runoff as the effective impervious surface (EIS). From Fig. 4, the EIS of DCL watershed experienced significant expansion from 2001 to 2018. From the perspective of time change, the effective ISA in 2018 is 2.1 times of that in 2001, and the growth rate of the effective impervious surface area (EISA) in the DCL watershed reaches 155.06 km^2 /decade (significance level $p < 0.01$). In terms of spatial transformation, prior to 2001, the EIS in the DCL watershed was concentrated mainly in the primary urban area north of DCL in Kunming. However, over time, the EIS that generates effective runoff in the DCL watershed has progressively spread towards the north of DCL's banks and along the south of the DCL's east bank. By 2018, the EISA that can produce effective runoff in the DCL watershed has reached 429.97 km^2, and the EIS in several sub-watersheds on the east bank of the DCL has also taken a large proportion.

3.2. Comparison between actual impervious surface and effective impervious surface

From Fig. 5, it can be observed that in all years, both the area and the yearly increment of actual IS exceed those of EIS. From the actual change of each year, the maximum difference between the two is in 2018, with the difference of 156.54 km^2. From the increment of each year, 2011 is the year with the fastest growth of IS, and the difference between the two also reaches 11.67 km^2.

3.3. Influence of near-surface air temperature change on lake surface water temperature

Fig. 6 shows the warming of LSWT caused by urban expansion in the DCL watershed through NSAT. From the figure, it can be seen that the actual warming trend in each year in the watershed is similar to the growth of ISA in the watershed, of which the warming in

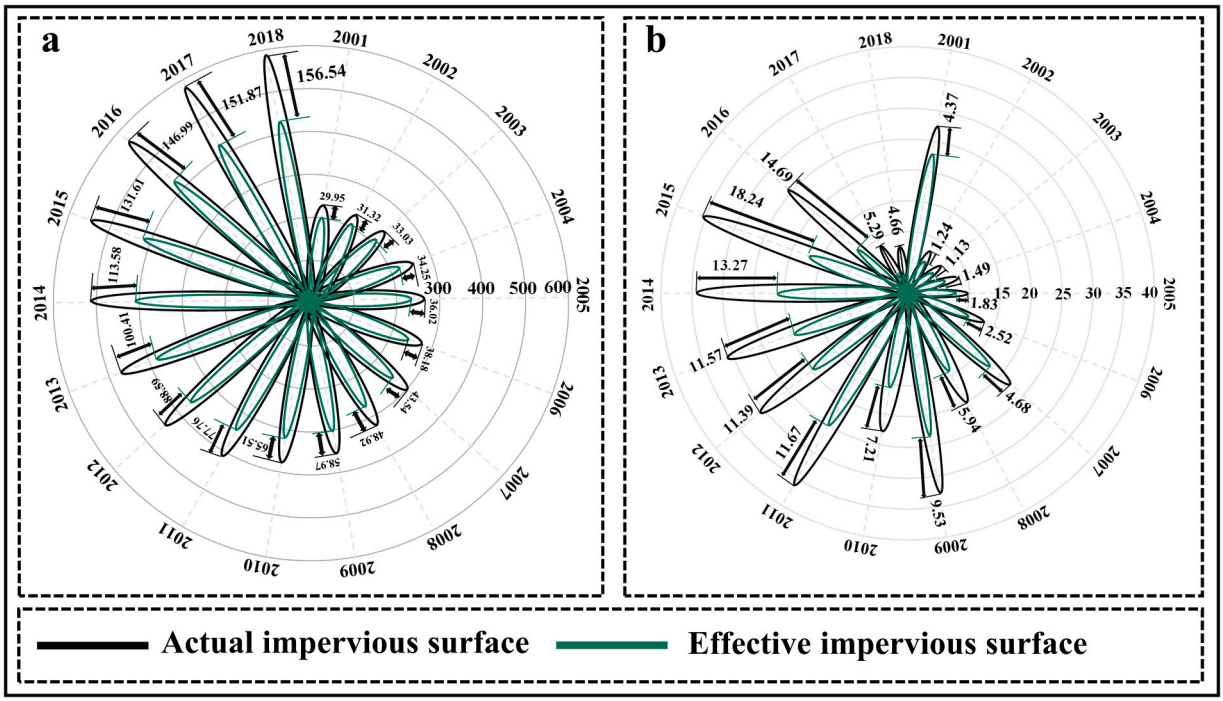

Fig. 5. Change of actual impervious surface and effective impervious surface. Note: Fig. a shows the area of the actual IS and the EIS in each year, and the number shows the difference between the two. The Fig. b shows the annual increment of the IS and the EIS, and the number shows the difference between the two.

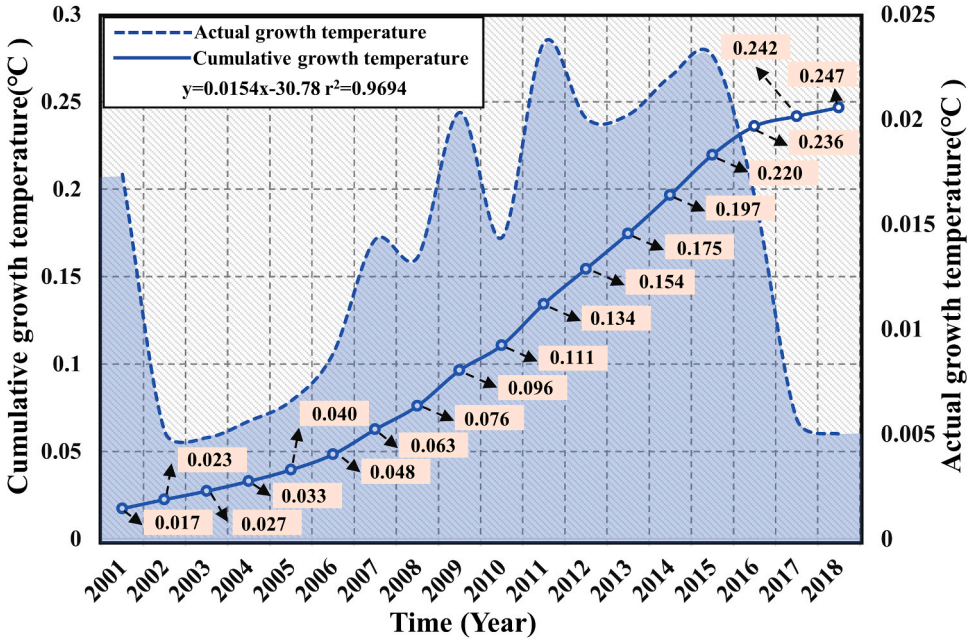

Fig. 6. The effect of near-surface air warming on lake surface water temperature.

2001 was relatively large, and the warming in each year after 2002 gradually increased, showing a downward trend after 2015. From the perspective of cumulative warming, urban expansion in the watershed has led to a significant increase of LSWT, with an increase trend of 0.15 °C /decade. From 2001–2018, the expansion of the cities in the DCL watershed increased the NSAT, resulting in a cumulative increase of the LSWT of about 0.25 °C.

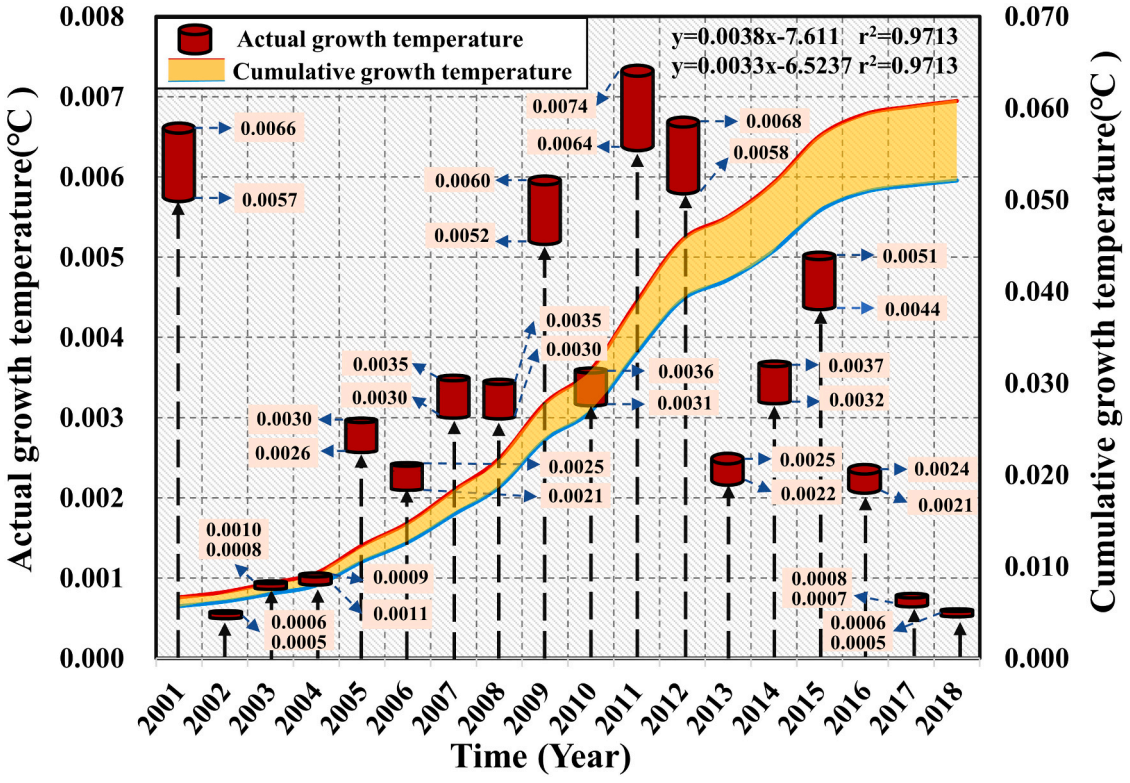

Fig. 7. Increase of lake surface water temperature by thermal runoff.

3.4. Increase of lake surface water temperature by thermal runoff

Fig. 7 shows the warming trend of LSWT attributed to the urban expansion in the DCL watershed through thermal runoff. From the actual growth temperature in each year, the increase in water temperature gradually increased after 2002, with 2011 being the year with the highest temperature increase, with a temperature increase of 0.0064–0.0074 °C for the LSWT. From the perspective of cumulative warming, the warming of LSWT caused by urban expansion in the DCL watershed through thermal runoff shows a significant upward trend, with an increase trend of 0.033–0.038 °C /decade (significance level $p < 0.01$). The cumulative increase in LSWT due to the addition of IS from 2001 to 2018 is estimated to be between 0.05 and 0.06 °C.

4. Discussion

4.1. Parameter selection of lake surface water temperature increase due to urban expansion

For the conversion efficiency between NSAT and lake surface temperature (T_{surf}), we refer to the study of (Schmid et al., 2014), who estimated the impact of climate change predicted by six climate models on T_{surf} globally, and evaluated the interaction between different forcing variables, the sensitivity of T_{surf} to these variables, and the differences between climatic regions. In this study, the scholar did not use the T_{surf}, but used the lake surface equilibrium temperature (T_{eq}), that is, the temperature at which the lake surface net heat flux is zero under given meteorological conditions as the representative of the T_{surf}. In the discussion part, the author mentioned that for shallow lakes, that is, most of the lakes in the world, the T_{eq} is a good representative of the T_{surf} on the seasonal time scale. In addition, $\triangle T_{surf}$ is more representative of $\triangle T_{eq}$, because the systematic difference between T_{surf} and T_{eq} is largely offset by the difference between the future and the baseline scenario (Wilhelm et al., 2006). In this paper, we did not consider the increase of LSWT caused by the existing IS every year, but the increase of LSWT caused by the increase of IS every year compared with the previous year, that is, the increase of LSWT caused by $\triangle$ impervious surface. Therefore, it is reasonable to refer to the scholar's research. And Schmid et al. (2014) also concluded that $\triangle T_{eq}$ is about 80% of $\triangle T_{air}$ in tropical and temperate climates, and this value is also referenced when calculating the energy conversion between air temperature and T_{surf} according to the location of the study area. The research results of Woolway et al. (2017)also show that the increased value of LSWT is about 80% of the increased value of air temperature.

The selection of research scales is of great significance for the impact of urban expansion on the warming of NSAT. Here, we choose the sub-watershed scale. The main reason for choosing the sub-watershed scale is that from the perspective of the spatial distribution of the IS of the DCL watershed, the cities in the DCL watershed are mainly distributed in the main urban area of Kunming on the north bank of the DCL. With the acceleration of the urbanization process in Kunming, the urban expansion in the DCL watershed extends southward along the east bank of the DCL (Luo et al., 2018). Apart from the sub-watersheds along the coast, the rate of urbanization in other sub-watersheds is comparatively low, with a relatively gradual pace of urban development. If participating in the calculation at the entire watershed scale, the impact of a large expanse of IS in the coastal region on urban expansion would be minimized, while the impact of a smaller area of IS in the distant regions on the LSWT would be overemphasized.

For the mixing of thermal runoff and DCL water, we directly use the amount of effective runoff and the capacity of DCL to calculate. Due to the fact that the research season is in summer and DCL is a shallow lake, it is not necessary to consider the stratification of DCL when calculating the warming effect of thermal runoff on the LSWT. Therefore, this paper directly uses the effective runoff and the capacity of DCL to calculate the water temperature.

4.2. Comparison between the warming of near-surface air temperature and the warming of thermal runoff on lake surface water temperature

By comparing the contribution of NSAT and thermal runoff to the warming of LSWT, it can be seen that the impact of urban expansion on LSWT through NSAT is significantly greater than that of thermal runoff on LSWT. The main reasons are as follows: first, for the increase of NSAT, as long as the new IS is added, it will have an effective impact on the NSAT. In contrast, there are relatively strict conditions for the IS that can generate thermal runoff, because the spatial relationship between the IS and the permeable surface will greatly affect the amount of effective runoff. Therefore, as shown in Fig. 4, the actual IS that affects the near surface, whether in terms of annual increments or total area, is much larger than the EIS that affects the thermal runoff. In addition, the conditions for the formation of thermal runoff are relatively stringent. In this paper, we use the cloud amount of the hour before rainfall as a reference. Rainfall during this period can be considered as part of the effective runoff only if the hour before rainfall is classified as cloudy or sunny weather. At the same time, some of the rainfall falling on the IS will be infiltrated when it flows through the permeable surface. Despite the fact that rainfall falling on the IS cannot flow to surrounding permeable surfaces for infiltration, a portion of the rainfall is still lost through evaporation and infiltration as it moves through the IS (Ramier et al., 2011).

4.3. Impact of urban expansion on lake surface water temperature rise and prevention and control measures

DCL is the sixth largest freshwater lake in China and the largest plateau lake on the Yunnan-Guizhou Plateau. Due to the impact of human activities, the water quality of DCL has deteriorated (Jia et al., 2023; Yang et al., 2018). Research results of some scholars indicated that most of the water quality indicators in DCL were significantly affected by the LSWT. Studies also found that LSWTs fundamentally affect lake cyanobacterial blooms(Yang et al., 2018). Hence, it is imperative to explore the means of controlling the

warming effect on LSWT resulting from the urban expansion. For the increase in NSAT, increasing vegetation area will have a significant cooling effect on NSAT and air temperature (Klok et al., 2012; Mathew et al., 2018). Optimizing the composition and configuration of landscape patterns within the region will also effectively reduce land surface temperature (Sun and Chen, 2012; Zhao et al., 2020b), thereby reducing the warming of NSAT on IS. The decrease in land surface temperature will also effectively reduce the temperature of thermal runoff, thereby reducing the increase in LSWT caused by urban expansion. In addition, the urban heat island can be improved by changing the materials of roof and pavement and selecting cool roof and pavement (Akbari and Kolokotsa, 2016; Tan and Wang, 2023). For thermal runoff, it can be alleviated through the construction of 'Sponge City'. The Sponge City was initially established to solve urban water management problems such as urban surface water flooding, urban runoff purification, flood peak runoff reduction and water conservation (Chan et al., 2018; Jiang et al., 2018). The DCL watershed is currently witnessing the development of numerous structures as part of the construction of a Sponge city. Substantial investments have been made in the future planning of the Sponge city project (https: //www.km. gov.cn /c /2022–12–14 /4612250. shtml). At the same time, infrastructure projects such as permeable pavement can also effectively reduce thermal runoff (Chan et al., 2018).

5. Conclusion

This paper studies the warming of LSWT during urban expansion from the perspectives of NSAT and thermal runoff. The results of this analysis offer valuable insights into the factors that influence the LSWT and can be used as a reference for urban planning process. Specific conclusions are as follows:

(1) From the perspective of time change, the IS in the DCL watershed experienced a significant expansion from 2001 to 2018, with a growth rate of 237.29 km^2 /decade (significance level $p < 0.01$), of which the EIS that can produce effective runoff has a growth rate of 155.06 km^2 /decade (significance level $p < 0.01$). From the perspective of spatial change, the IS was mainly distributed in the main urban area of Kunming in 2001, and then expanded along the main urban area to the north bank of DCL and along the east bank of DCL to the south.
(2) From the perspective of the impact of urban expansion in the DCL watershed on the LSWT by increasing the NSAT, the annual warming change is similar to the increase of the ISA, with the largest annual increase in 2011. The increase in the LSWT of the newly added IS in that year was 0.024 °C. From 2001–2018, the new IS of DCL increased the LSWT by about 0.25 °C by increasing the NSAT.
(3) From the perspective of the impact of urban expansion in the DCL watershed on the LSWT through thermal runoff, the annual increase is also similar to the increase of ISA. In 2001, the increase of LSWT through thermal runoff was between 0.006 and 0.007. From 2001–2018, the cumulative increase in LSWT caused by the newly increased IS in the DCL watershed through thermal runoff was about 0.05–0.06 °C.
(4) By comparing the increase of NSAT and thermal runoff on the LSWT, it can be seen that the impact of urban expansion on the LSWT is mainly through the increase of NSAT.
(5) Based on the integration of relevant fields and the research achievements of our team, this article innovatively proposes a method that can effectively quantify the specific increase in LSWT caused by urban expansion, considering the mechanisms of urban expansion's impact on LSWT. The experimental results demonstrate that this method is able to effectively quantify the specific temperature increase on the LSWT caused by urban expansion.
(6) From the results of the studies, we conclude that a viable approach to reduce the impact of urban expansion on LSWT is to optimize the landscape pattern, strategically arrange buildings and vegetation within the city, and choose suitable building materials.

CRediT authorship contribution statement

Yi Luo: Conceptualization, Resources, Funding acquisition, Writing – review & editing. **Linfeng Tang:** Methodology, Validation, Writing – original draft. **Kun Yang:** Conceptualization, Resources. **Xiaolu Zhou:** Writing – review & editing. **Jing Liu:** Data processing. **Yang Zhang:** Data processing. **Zongqi Peng:** Data processing.

Declaration of Competing Interest

The authors declare that they have no known competing financial interests or personal relationships that could have appeared to influence the work reported in this paper.

Data Availability

Data will be made available on request.

Acknowledgements

This study was financially supported by the National Natural Science Foundation of China (grant numbers:42271441); the Ten Thousand Talent Plans for Young Top-notch Talents of Yunnan Province (grant numbers: YNWR-QNBJ-2019-200); and the Graduate

Research Innovation Fund of Yunnan Normal University (grant numbers: YJSJJ22-B105).

References

Akbari, H., Kolokotsa, D., 2016. Three decades of urban heat islands and mitigation technologies research. Energy Build. 133, 834–842. https://doi.org/10.1016/j.enbuild.2016.09.067.

Austin, J.A., Colman, S.M., 2007. Lake Superior summer water temperatures are increasing more rapidly than regional air temperatures: a positive ice-albedo feedback. Geophys. Res. Lett. 34 (6), 5. https://doi.org/10.1029/2006gl029021.

Buren, M.A.V., Watt, W.E., Marsalek, J., 2000. Thermal enhancement of stormwater runoff by paved surfaces. Water Res. 34 (4), 1359–1371.

Chan, F.K.S., et al., 2018. "Sponge City" in China-a breakthrough of planning and flood risk management in the urban context. Land Use Pol. 76, 772–778. https://doi.org/10.1016/j.landusepol.2018.03.005.

Chen, K.L., Wang, X., Li, D., Li, Z.H., 2015. Driving force of the morphological change of the urban lake ecosystem: a case study of Wuhan, 1990-2013. Ecol. Model. 318, 204–209. https://doi.org/10.1016/j.ecolmodel.2015.06.017.

Chen, Y.X., Huang, B.Y., Zeng, H., 2022. How does urbanization affect vegetation productivity in the coastal cities of eastern China. Sci. Total Environ. 811, 10. https://doi.org/10.1016/j.scitotenv.2021.152356.

Debbage, N., Shepherd, J.M., 2015. The urban heat island effect and city contiguity. Comput. Environ. Urban Syst. 54, 181–194. https://doi.org/10.1016/j.compenvurbsys.2015.08.002.

Du, J., et al., 2020a. Monitoring of water surface temperature of Eurasian large lakes usingMODISland surface temperature product. Hydrol. Process. 34 (16), 3582–3595. https://doi.org/10.1002/hyp.13830.

Du, J., Xiang, X.Y., Zhao, B.Y., Zhou, H.H., 2020b. Impact of urban expansion on land surface temperature in Fuzhou, China using landsat imagery. Sustain Cities Soc. 61, 15. https://doi.org/10.1016/j.scs.2020.102346.

Galli, J., 1990. Thermal Impacts Associated With Urbanization and Stormwater Best Management Practices. Metropolitan Washington Council of Governments, Washington, DC. 188 pp.

Gong, P., et al., 2020. Annual maps of global artificial impervious area (GAIA) between 1985 and 2018. Remote Sens. Environ. 236, 12. https://doi.org/10.1016/j.rse.2019.111510.

Gu, C.L., 2019. Urbanization: positive and negative effects. Sci. Bull. 64 (5), 281–283. https://doi.org/10.1016/j.scib.2019.01.023.

Hampton, S.E., et al., 2008. Sixty years of environmental change in the world's largest freshwater lake - Lake Baikal, Siberia. Glob. Change Biol. 14 (8), 1947–1958. https://doi.org/10.1111/j.1365-2486.2008.01616.x.

Hawker, L., et al., 2022. A 30 m global map of elevation with forests and buildings removed. Environ. Res. Lett. 17 (2), 11. https://doi.org/10.1088/1748-9326/ac4d4f.

He, Y.T., Jia, G.S., Hu, Y.H., Zhou, Z.J., 2013. Detecting urban warming signals in climate records. Adv. Atmos. Sci. 30 (4), 1143–1153. https://doi.org/10.1007/s00376-012-2135-3.

Herb, W.R., Janke, B., Mohseni, O., Stefan, H.G., 2008. Thermal pollution of streams by runoff from paved surfaces. Hydrol. Process. 22 (7), 987–999. https://doi.org/10.1002/hyp.6986.

Hersbach, H., et al., 2020. The ERA5 global reanalysis. Q. J. R. Meteorol. Soc. 146 (730), 1999–2049. https://doi.org/10.1002/qj.3803.

Houser, J.N., 2006. Water color affects the stratification, surface temperature, heat content, and mean epilimnetic irradiance of small lakes. Can. J. Fish. Aquat. Sci. 63 (11), 2447–2455. https://doi.org/10.1139/f06-131.

Huziy, O., Sushama, L., 2017. Impact of lake-river connectivity and interflow on the Canadian RCM simulated regional climate and hydrology for Northeast Canada. Clim. Dyn. 48 (3–4), 709–725. https://doi.org/10.1007/s00382-016-3104-9.

Janke, B.D., Herb, W.R., Mohseni, O., Stefan, H.G., 2009. Simulation of heat export by rainfall-runoff from a paved surface. J. Hydrol. 365 (3–4), 195–212. https://doi.org/10.1016/j.jhydrol.2008.11.019.

Jia, L., Zhou, Q., Li, Y., Wu, W., 2023. Integrated treatment of suburb diffuse pollution using large-scale multistage constructed wetlands based on novel solid carbon: nutrients removal and microbial interactions. J. Environ. Manag. 326 (B), 116709 https://doi.org/10.1016/j.jenvman.2022.116709.

Jia, T.F., et al., 2022. Review on the change trend, attribution analysis, retrieval, simulation, and prediction of lake surface water temperature. IEEE J. Sel. Top. Appl. Earth Obs. Remote Sens. 15, 6324–6355. https://doi.org/10.1109/jstars.2022.3188788.

Jiang, Y., Zevenbergen, C., Ma, Y.C., 2018. Urban pluvial flooding and stormwater management: a contemporary review of China's challenges and "sponge cities" strategy. Environ. Sci. Policy 80, 132–143. https://doi.org/10.1016/j.envsci.2017.11.016.

Jiao, D.L., Xu, N.N., Yang, F., Xu, K., 2021. Evaluation of spatial-temporal variation performance of ERA5 precipitation data in China. Sci. Rep. 11 (1), 13. https://doi.org/10.1038/s41598-021-97432-y.

Kim, J.Y., Sansalone, J.J., 2008. Zeta potential of clay-size particles in urban rainfall-runoff during hydrologic transport. J. Hydrol. 356 (1–2), 163–173. https://doi.org/10.1016/j.jhydrol.2008.04.006.

Klok, L., Zwart, S., Verhagen, H., Mauri, E., 2012. The surface heat island of Rotterdam and its relationship with urban surface characteristics. Resour. Conserv. Recycl. 64, 23–29. https://doi.org/10.1016/j.resconrec.2012.01.009.

Liu, C., Xiao, W., Zeng, Y., Li, H.J., 2022. Diurnal variation characteristics of temoerature in jiangxi under different weather backgrounds. meteorology and disaster reduction. Research 45 (02), 114–124.

Luo, Y., et al., 2017. Dynamic monitoring and prediction of Dianchi Lake cyanobacteria outbreaks in the context of rapid urbanization. Environ. Sci. Pollut. Res. 24 (6), 5335–5348. https://doi.org/10.1007/s11356-016-8155-2.

Luo, Y., et al., 2018. Dianchi Lake watershed impervious surface area dynamics and their impact on lake water quality from 1988 to 2017. Environ. Sci. Pollut. Res. 25 (29), 29643–29653. https://doi.org/10.1007/s11356-018-2967-1.

Luo, Y., et al., 2019. Thermodynamic analysis of air-ground and water-ground energy exchange process in urban space at micro scale. Sci. Total Environ. 694, 13. https://doi.org/10.1016/j.scitotenv.2019.133612.

Luo, Y., Zhang, Y., Yang, K., Zhou, X.L., Peng, Z.Q., 2023. Urban surface thermal runoff generation mechanism and scenario simulation. Water Resour. Res. 59 (4), 19. https://doi.org/10.1029/2022wr033881.

Martinez-Zarzoso, I., Maruotti, A., 2011. The impact of urbanization on CO_2 emissions: evidence from developing countries. Ecol. Econ. 70 (7), 1344–1353. https://doi.org/10.1016/j.ecolecon.2011.02.009.

Mathew, A., Khandelwal, S., Kaul, N., 2018. Analysis of diurnal surface temperature variations for the assessment of surface urban heat island effect over Indian cities. Energy Build. 159, 271–295. https://doi.org/10.1016/j.enbuild.2017.10.062.

O'Reilly, C.M., Alin, S.R., Plisnier, P.D., Cohen, A.S., McKee, B.A., 2003. Climate change decreases aquatic ecosystem productivity of Lake Tanganyika, Africa. Nature 424 (6950), 766–768. https://doi.org/10.1038/nature01833.

Peng, Z.Q., et al., 2022. Attribution analysis of lake surface water temperature changing -taking China's six main lakes as example. Ecol. Indic. 145, 12. https://doi.org/10.1016/j.ecolind.2022.109651.

Ptak, M., Sojka, M., Choinski, A., Nowak, B., 2018. Effect of environmental conditions and morphometric parameters on surface water temperature in Polish Lakes. Water 10 (5). https://doi.org/10.3390/w10050580.

Ramier, D., Berthier, E., Andrieu, H., 2011. The hydrological behaviour of urban streets: long-term observations and modelling of runoff losses and rainfall-runoff transformation. Hydrol. Process. 25 (14), 2161–2178. https://doi.org/10.1002/hyp.7968.

Sabouri, F., Gharabaghi, B., Mahboubi, A.A., McBean, E.A., 2013. Impervious surfaces and sewer pipe effects on stormwater runoff temperature. J. Hydrol. 502, 10–17. https://doi.org/10.1016/j.jhydrol.2013.08.016.

Schmid, M., Koster, O., 2016. Excess warming of a Central European lake driven by solar brightening. Water Resour. Res. 52 (10), 8103–8116. https://doi.org/10.1002/2016wr018651.
Schmid, M., Hunziker, S., Wuest, A., 2014. Lake surface temperatures in a changing climate: a global sensitivity analysis. Clim. Change 124 (1–2), 301–315. https://doi.org/10.1007/s10584-014-1087-2.
Sharma, S., Jackson, D.A., Minns, C.K., Shuter, B.J., 2007. Will northern fish populations be in hot water because of climate change. Glob. Change Biol. 13 (10), 2052–2064. https://doi.org/10.1111/j.1365-2486.2007.01426.x.
Sun, D.Q., et al., 2017. New-type urbanization in China: predicted trends and investment demand for 2015-2030. J. Geogr. Sci. 27 (8), 943–966. https://doi.org/10.1007/s11442-017-1414-4.
Sun, R.H., Chen, L.D., 2012. How can urban water bodies be designed for climate adaptation. Landsc. Urban Plan. 105 (1–2), 27–33. https://doi.org/10.1016/j.landurbplan.2011.11.018.
Tan, K.H., Wang, J.S., 2023. Substrate modified with biochar improves the hydrothermal properties of green roofs. Environ. Res. 216, 12. https://doi.org/10.1016/j.envres.2022.114405.
Tang, L., Yang, K., Shang, C., Peng, Z., Luo, Y.J.Fi.E.S., 2022. Spatial impact of urban expansion on lake surface water temperature based on the perspective of watershed scale. 1503.
Tarek, M., Brissette, F.P., Arsenault, R., 2020. Evaluation of the ERA5 reanalysis as a potential reference dataset for hydrological modelling over North America. Hydrol. Earth Syst. Sci. 24 (5), 2527–2544. https://doi.org/10.5194/hess-24-2527-2020.
Wilhelm, S., Hintze, T., Livingstone, D.M., Adrian, R., 2006. Long-term response of daily epilimnetic temperature extrema to climate forcing. Can. J. Fish. Aquat. Sci. 63 (11), 2467–2477. https://doi.org/10.1139/f06-140.
Woolway, R.I., et al., 2017. Warming of Central European lakes and their response to the 1980s climate regime shift. Clim. Change 142, 505–520.
Woolway, R.I., et al., 2019. Substantial increase in minimum lake surface temperatures under climate change. Clim. Change 155 (1), 81–94. https://doi.org/10.1007/s10584-019-02465-y.
Woolway, R.I., Jennings, E., Carrea, L., 2020. Impact of the 2018 European heatwave on lake surface water temperature. Inland Waters 10 (3), 322–332. https://doi.org/10.1080/20442041.2020.1712180.
Xu, L., Wang, J.Y., Xiao, F.P., Ei-Badawy, S., Awed, A., 2021. Potential strategies to mitigate the heat island impacts of highway pavement on megacities with considerations of energy uses. Appl. Energy 281, 27. https://doi.org/10.1016/j.apenergy.2020.116077.
Yang, K., et al., 2018. Spatial and temporal variations in the relationship between lake water surface temperatures and water quality - a case study of Dianchi Lake. Sci. Total Environ. 624, 859–871. https://doi.org/10.1016/j.scitotenv.2017.12.119.
Yang, K., et al., 2020a. Spatial-temporal variations in urbanization in Kunming and their impact on urban lake water quality. Land Degrad. Dev. 31 (11), 1392–1407. https://doi.org/10.1002/ldr.3543.
Yang, K., Yu, Z.Y., Luo, Y., Zhou, X.L., Shang, C.X., 2019. Spatial-temporal variation of lake surface water temperature and its driving factors in Yunnan-Guizhou plateau. Water Resour. Res. 55 (6), 4688–4703. https://doi.org/10.1029/2019wr025316.
Yang, K., Yu, Z.Y., Luo, Y., 2020b. Analysis on driving factors of lake surface water temperature for major lakes in Yunnan-Guizhou Plateau. Water Res. 184, 9. https://doi.org/10.1016/j.watres.2020.116018.
Yang, K., Zhang, Y., Luo, Y., Shang, C.X., 2021. Precipitation events impact on urban lake surface water temperature under the perspective of macroscopic scale. Environ. Sci. Pollut. Res. 28 (13), 16767–16780. https://doi.org/10.1007/s11356-020-12093-0.
Yao, F., Zhu, H.S., Wang, M.J., 2021. The impact of multiple dimensions of urbanization on CO_2 emissions: a spatial and threshold analysis of panel data on China's prefecture-level cities. Sust. Cities Soc. 73, 13. https://doi.org/10.1016/j.scs.2021.103113.
Yu, Z., 2022. Study on the Attribution of Lake Surface Water Temperature Change and the Key Technology and Theory of Predicting its Spatio-temporal Change Trend - A Case Study of Nine Plateau Lakes in Yunnan Province. Yunnan Normal University. https://doi.org/10.27459/d.cnki.gynfc.2022.000005.
Zhao, B.Y., et al., 2020a. Spatio-temporal variation of water heat flux using MODIS land surface temperature product over Hulun Lake, China During 2001-2018. Chin. Geogr. Sci. 30 (6), 1065–1080. https://doi.org/10.1007/s11769-020-1166-4.
Zhao, J.C., et al., 2020b. Assessing the thermal contributions of urban land cover types. Landsc. Urban Plan. 204, 11. https://doi.org/10.1016/j.landurbplan.2020.103927.
Zhou, D.C., Zhao, S.Q., Liu, S.G., Zhang, L.X., Zhu, C., 2014. Surface urban heat island in China's 32 major cities: spatial patterns and drivers. Remote Sens. Environ. 152, 51–61. https://doi.org/10.1016/j.rse.2014.05.017.